J Toxicol Pathol 2022; 35: 321–331

Original Article

Chemical-induced lung tumor in Tg-rasH2 mice: a novel mouse tumor model to assess immune checkpoint inhibitors combined with a chemotherapy drug

Teruaki Hagiwara[1*], Takamasa Numano[1], Tomomi Hara[1], Taiki Sugiyama[1], Yukinori Mera[1], Seiko Tamano[1], and Hiroto Miyata[1]

[1] DIMS Institute of Medical Science, Inc., 64 Goura, Nishiazai, Azai-cho, Ichinomiya-shi, Aichi 491-0113, Japan

Abstract: In subcutaneous tumor models, changes in the tumor microenvironment can lead to differences in therapeutic treatment responses between the subcutaneous and parent tumors. Accordingly, we generated a lung carcinogenesis model that combines genetically modified mice (Tg-rasH2 mice) with two-stage chemical carcinogenesis as an alternative to the subcutaneous tumor model. In this model, Tg-rasH2 mice were treated with 1-ethyl-1-nitrosourea, followed by butylhydroxytoluene. Mice developed lung adenomas five weeks after treatment initiation. Subsequently, anti-mouse PD-1 antibody (α-mPD-1) or isotype control was administered intraperitoneally twice a week for 4 weeks. Tumor growth was examined by measuring the relative tumor area in serially sliced lung histopathological specimens. No statistically significant differences were observed in the relative lung tumor areas between treated and control groups. A second experiment then examined the antitumor efficacy of α-mPD-1 combined with gemcitabine in a mouse model. Mice were treated identically as in Experiment 1, except that the treated group received once-weekly intraperitoneal injections of 10 mg/kg gemcitabine. In contrast to Experiment 1, the combined treatment significantly reduced the relative tumor areas in the lungs. This result also resembles that of a phase III clinical trial (ORIENT-12), showing that patients with non-small-cell lung carcinoma benefited from combination treatment with gemcitabine and the anti-human PD-1 antibody sintilimab. Thus, this mouse model could be a feasible means to preclinically evaluate the antitumor efficacy of different immunotherapy and chemotherapy drug combinations.
(DOI: 10.1293/tox.2022-0040; J Toxicol Pathol 2022; 35: 321–331)

Key words: immune checkpoint inhibitors (ICI), ICI therapy model, chemically-induced lung carcinogenesis, rasH2 mice, gemcitabine, PD-1

Introduction

Lung cancer is a leading cause of cancer-related deaths worldwide in both male and female patients[1]. Treatment outcomes are generally poor, with 5-year survival rates ranging from 4 to 17%, depending on the disease stage and region[2]. Immune checkpoint inhibitor (ICI) monotherapy for lung cancer has improved patient outcomes; however, the response rate remains low at approximately 20%[3]. Therefore, various combination therapies using existing chemotherapy drugs, both marketed or under development, and ICIs are under preclinical and clinical investigation. However, given the lack of suitable animal models for examining ICI-mediated antitumor effects, the success rate of drug discovery is poor. Therefore, specific preclinical models that can extrapolate preclinical antitumor efficacy to humans are required.

Mouse models for testing preclinical antitumor efficacy include xenograft models using cell lines or patient-derived tumor tissues (PDX), syngeneic tumor models, chemical carcinogenesis models, and genetically engineered mouse models. Each model has advantages and disadvantages, considering clinical predictive power and study duration. For example, xenograft models utilize human cancer cells or tumor tissues; therefore, responses to treatment are considered to reflect those of human tumors to the test treatment. However, these models have two major disadvantages. When mice are subcutaneously engrafted with human cancer cells or tumor tissue, the primary tumor microenvironment is dramatically altered, resulting in distinct therapeutic drug responses between the primary tumor and xenograft[4]. The second disadvantage of the xenograft model is the need for immunocompromised mice, leading to differences in therapeutic drug responses mediated by the primary tumor, thereby hindering the evaluation of immunotherapy agents[5]. Syngeneic tumor models utilize tumor tissues derived from the same genetic background as the tester mouse strain. Consequently, mice with intact immune systems are

Received: 22 March 2022, Accepted: 6 June 2022
Published online in J-STAGE: 26 June 2022
*Corresponding author: T Hagiwara (e-mail: teruaki@dims.co.jp)

employed; however, this model also uses mouse tumor cells and tissues. Furthermore, syngeneic tumor models involve subcutaneous implantation, resulting in a dramatically altered microenvironment from that in which the primary tumor develops, leading to differences in therapeutic drug responses between primary and syngeneic tumors[6]. In genetically engineered mouse models, tumorigenic driver mutations can be introduced, although simulating the complex genetic landscape of human tumors has not been achieved[7]. Considering the advantages of chemical carcinogenesis models, it is well accepted that chemicals that cause cancer in rodents are potential human carcinogens, suggesting that chemical carcinogenesis models in mice may reliably reflect tumorigenesis in humans. Chemicals that directly or indirectly induce mutations in mice can potentially cause mutations in humans. As tumorigenesis is initiated and driven by mutations, chemicals that cause mutations and are carcinogenic in mice are potential human carcinogens. However, specific genetic changes that lead to cancer development vary considerably between mice and humans. Deficiencies in the above-listed mouse models have resulted in most cancer treatments and drugs being successful in preclinical testing but failing in clinical trials[7, 8].

The Tg-rasH2 (hereafter referred to as rasH2) mouse, a genetically engineered mouse containing multiple copies of the human c-Ha-ras gene (HRAS), is considered a standard animal for short-term carcinogenicity studies, with a test period of approximately 6 months when compared with 2 years for the conventional method[9]. To induce a lung cancer model in this genetically engineered mouse, we performed a two-step chemical carcinogenesis protocol: initiation with 1-ethyl-1-nitrosourea (ENU) and promotion with butylhydroxytoluene (BHT). ENU, also known as N-ethyl-N-nitrosourea, ethylnitrosourea, and N-nitroso-N-ethylurea, is a well-known genotoxic carcinogen that induces tumor formation in experimental animals at several different tissue sites and via several different exposure routes[10, 11]. BHT promotes the proliferation of type II alveolar epithelial cells and has been shown to promote carcinogenesis initiated by several genotoxic compounds[12, 13]; however, both mice and rats were negative in a 2-year study examining the carcinogenicity of BHT[14]. As previously reported, initiation of ENU and promotion with BHT in rasH2 mice can result in a high incidence of lung tumors at 9 weeks[13].

Gemcitabine (GEM) is typically administered weekly at 1,000 or 1,250 mg/m^2 via a 30-min intravenous infusion for 2 or 3 weeks, followed by a 1-week rest period. As of 2009, the combination of GEM and cisplatin is the first-choice therapy for patients with advanced non-small-cell lung carcinoma (NSCLC). Moreover, pharmacoeconomic data revealed that this combination was the most cost-effective regimen among combination therapies with platinum and third-generation cytotoxic drugs[15]. A large body of evidence supports the close association between myeloid-derived suppressor cell (MDSC) accumulation and clinical outcomes in patients with lung cancer[16]. MDSCs accumulate in the spleen and tumor bed during tumor growth. *In vivo*, compared with oxaliplatin, a cisplatin analogue, GEM showed significant selective cytotoxicity against tumor and spleen MDSCs[17]. The combination of GEM and ICI outperformed immunotherapy alone with regard to tumor control and survival in a preclinical mesothelioma model[18]. Therefore, given the mechanism of action of anti-PD-1 antibodies (ICIs), the current study investigated the antitumor effect based on the hypothesis that the combined administration of anti-PD-1 antibodies and GEM could afford a synergistic effect in a lung chemical carcinogenesis model.

Materials and Methods

Chemicals and reagents

ENU was purchased from Sigma-Aldrich (St Louis, MO, USA), and BHT and GEM were purchased from Tokyo Chemical Industry Co., Ltd. (Tokyo, Japan). Anti-mouse PD-1 (CD279) antibody (α-mPD-1) (clone: RMP1-14) and rat IgG2a (clone:2A3), used as isotype controls, were purchased from Bio X Cell (Lebanon, NH, USA).

Animals, animal husbandry, and establishment of the lung tumor model

The present study was approved by the Animal Experimental Committee at the DIMS Institute of Medical Science, Inc. on a protocol basis (Control No. 19558, 20530) and conducted in accordance with the "Law for the Humane Treatment and Management of Animals" (Law No. 39, June 2019), "Standards Relating to the Care and Management of Laboratory Animals and Relief of Pain" (Notice No. 84 of the Ministry of the Environment, September 2013), "Guidelines for Proper Conduct of Animal Experiments" (Science Council of Japan, June 2006), and "Standards for Care and Use of Laboratory Animals of DIMS Institute of Medical Science, Inc." (1 October 2019).

Herein, we used six-week-old female CByB6F1-Tg(HRAS)2Jic mice, hereafter referred to as rasH2 mice, purchased from CLEA Japan, Inc. (Tokyo, Japan), owing to the efficient and early development of lung tumors in these mice[13]. The animals were housed in a barrier-system animal room maintained under controlled conditions (temperature, 22 ± 3°C; humidity, 55 ± 15%; 12-h light-dark cycle) and provided a pellet diet MF (Oriental Yeast Co., Tokyo, Japan) and water *ad libitum*.

The lung tumor model was established as previously described[12, 13]. Briefly, after a one-week quarantine and acclimatization period, seven-week-old rasH2 mice were administered a single intraperitoneal (i.p.) injection (10 mL/kg) of a saline solution of 12 mg/mL ENU to initiate tumorigenesis in the lung. One week later, a corn oil suspension of 40 mg/mL BHT was orally administered to mice (10 mL/kg) once weekly for five weeks to promote lung tumorigenesis, as shown in Fig. 1A. The animals were randomized by body weight and assigned to groups one day before initiating experimental treatments.

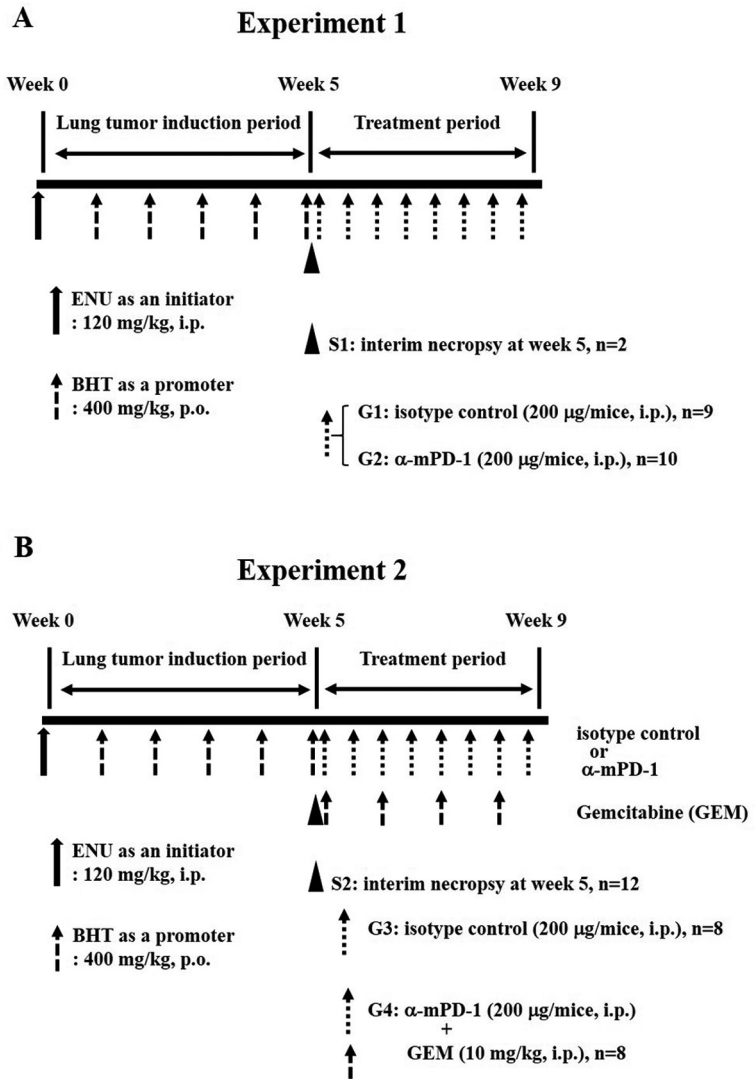

Fig. 1. Experimental designs. Groups and treatment schedules in Experiment 1 are shown in Panel A. Tumorigenesis was initiated by administering an intraperitoneal (i.p.) injection of ENU and promoted by oral administering BHT. After confirming the development of nodular masses in the lung of S1 mice, mice in G1 and G2 were treated with i.p. injections of isotype control or α-mPD-1, respectively. Groups and treatment schedules in Experiment 2 are shown in Panel B. Tumorigenesis was initiated by administering an i.p. injection of ENU and promoted by orally administering BHT, as in Experiment 1. After confirming the development of nodular masses in the lung of S2 mice, mice in G3 and G4 were treated with i.p. injections of isotype control or α-mPD-1, respectively. Mice in G4 were also treated with i.p. injections of GEM. α-mPD-1, anti-mouse PD-1 antibody; BHT, butylhydroxytoluene; ENU, 1-ethyl-1-nitrosourea; GEM, gemcitabine.

Treatment of lung carcinogenesis model mice with α-mPD-1 (Experiment 1) and α-mPD-1 and GEM combination (Experiment 2)

In Experiment 1, 22 lung tumor model mice, generated by treatment with ENU and BHT as described above, were randomized and allocated into three groups consisting of 10 mice in control and treated groups (Group 1: G1 and Group 2: G2, respectively) and two mice in the untreated group (Satellite group 1: S1) to confirm tumor expression at week 5 (the fifth week after carcinogen administration). After confirming nodular mass formation, mice in Groups 1 and 2 received i.p. injections of isotype control and α-mPD-1 (200 μg/mouse), respectively, twice a week for 4 weeks (Fig. 1A). The administration conditions of α-mPD-1, including dose and interval, were as previously reported[19–23].

In Experiment 2, a total of 28 lung tumor model mice were randomized and allocated into three groups consisting of 8 mice in control and treated groups (Groups 3: G3 and Group 4: G4, respectively) and 12 mice in the untreated group (Satellite Group 2: S2); mice in S2 group were subjected to gross pathology at the week 5 interim necropsy to confirm nodular mass formation in the lung. After confirming nodular mass formation, mice in Groups 3 and 4 received i.p. injections of isotype control and α-mPD-1 (200 μg/mice), respectively, twice a week for 4 weeks. In addition, mice in group 4 received concomitant i.p. injections of a saline solution of GEM (10 mg/kg) once weekly (Fig. 1B). The GEM administration conditions, including dose and interval, followed those previously reported[18, 24].

Examinations

The animals were observed for clinical signs, including general behaviour and symptoms, twice daily throughout the experimental period. Animals were weighed on the day of ENU administration and subsequently twice weekly.

Following isoflurane inhalation anesthesia and exsanguination from the abdominal aorta, gross pathology of all organs and tissues was examined at necropsy. The lung and other gross lesions were preserved in a 10% buffered formalin solution.

For histopathology, all lung lobes, including the bronchus, were sliced into 5 mm-thick serial sections embedded in paraffin and processed for hematoxylin and eosin (H&E) staining and histopathological examination. To verify the potential tumor responsiveness to α-mPD-1, lung tissue sections of mice were stained with anti-PD-L1 (programmed death-ligand 1) antibody (clone: D5V3B, #64988; Cell Signaling Technology Inc., Danvers, MA, USA) and visualized using the polymer method (Envision™Single Reagents, Envision™+/HRP, RUO).

Image analysis was conducted using H&E-stained serial sections from each lung lobe (approximately 22 sections per mouse) with a digital microscope, VHX-5000 (Keyence Corporation, Osaka, Japan). The relative tumor area per cm^2 lung tissue was then calculated.

Statistical analysis

To determine significant differences in the relative tumor area between the isotype control and ICI-treated groups (α-mPD-1 monotherapy or α-mPD-1 plus GEM combination therapy), the homogeneity of the variance among groups was tested using the F-test. The Student's t-test was used when the variance was homogenous; for heterogeneous variance, the Aspin–Welch's t-test was used. P was set at $p<0.05$.

Results

Treatment of lung carcinogenesis model mice with α-mPD-1 alone (Experiment 1)

At interim necropsy performed at week 5, we confirmed the presence of macroscopic lung nodular masses in the two S2 Tg-rasH2 mice treated with ENU and BHT. Histopathological examination of H&E-stained sections revealed adenomas in the lungs of the two untreated mice (S1) at week 5 (Table 1). No mortality was reported during the study period. Moreover, no notable clinical signs and body weight changes were documented between the isotype control and α-mPD-1 groups (Table 2). At the study endpoint (week 9), the tumor area was reduced in mice treated with α-mPD-1 when compared with isotype control mice; however, the difference was not statistically significant (3.15 and 2.54 mm^2/cm^2 in isotype control and α-mPD-1 treated mice, respectively) (Fig. 2, Table 3).

Treatment of lung carcinogenesis model mice with a combination of α-mPD-1 and GEM (Experiment 2)

No mortality was documented during the study period. In addition, no notable clinical signs and body weight chang-

Table 1. Incidence and Multiplicity of Lung Hyperplasia and Adenoma

Expt.	Group	Treatment	No. of mice	No. of Lung section examined	Necropsy at week	Hyperplasia		Adenoma	
						Incidence (%)	No. of foci	Incidence (%)	No. of foci
1	S1	-	2	-[a]	5	-[a]	-[a]	2 (100)	-[a]
	G1	Isotype control	9	21.6 ± 0.7[b]	9	4 (44)	0.89 ± 1.62[b]	9 (100)	8.22 ± 3.15[b]
	G2	α-mPD-1	10	21.8 ± 0.4	9	4 (40)	0.80 ± 1.03	10 (100)	9.20 ± 3.33
2	S2	-	12	22.0 ± 0.4	5	10 (83)	2.08 ± 1.68	12 (100)	6.25 ± 2.42
	G3	Isotype control	8	21.6 ± 0.9	9	3 (38)	0.38 ± 0.52	8 (100)	14.50 ± 2.73
	G4	α-mPD-1 + GEM	8	22.1 ± 0.4	9	8 (100)	2.00 ± 1.31	8 (100)	11.13 ± 2.80*

a: Only tumor expression was confirmed, b: Mean ± SD. *$p<0.05$ compared to Group 3 with Student's t-test.
All mice were administered ENU+BHT as initiation/promotion protocol.

Table 2. Body Weight Change during Experiments 1 and 2

Expt.	Groups	Treatment	No. of mice	Lung tumor induction period; ENU/BHT administration			Treatment period	
				Week 0	Week 5	Weight gain (Week 0 to 5)	Week 9	Weight gain (Week 5 to 9)
1	S1	-	2	19.8 ± 0.1[a]	22.0 ± 2.7	2.2 ± 2.2	-	-
	G1	Isotype control	9	19.6 ± 0.7	20.7 ± 1.5	1.0 ± 1.6	21.8 ± 0.9	1.1 ± 1.0
	G2	α-mPD-1	10	19.1 ± 0.8	20.5 ± 0.9	2.8 ± 1.2	21.9 ± 1.1	1.4 ± 0.9
2	S2	-	12	18.2 ± 0.9	19.8 ± 0.6	1.6 ± 0.8	-	-
	G3	Isotype control	8	17.8 ± 0.8	19.5 ± 0.6	1.7 ± 0.8	21.6 ± 1.0	2.1 ± 0.6
	G4	α-mPD-1 + GEM	8	17.5 ± 1.1	19.6 ± 0.8	2.2 ± 0.9	21.6 ± 1.4	1.9 ± 1.0

a: Mean ± SD (g).

es were noted between the isotype control and α-mPD-1 and GEM combination groups (Table 2). The body weights of all animals were within the range of the facility background data for this model. Based on the results, treatment with α-mPD-1 in combination with GEM did not impact the body weight. There were no gross pathological findings, except for nodular lung masses (Fig. 3).

As in Experiment 1, at the 5-week interim necropsy, we confirmed the presence of macroscopic nodular masses (Fig. 3) in the lungs of S2 mice treated with ENU and BHT. These masses were observed in all 12 mice and were confirmed to be adenomas by microscopic examination of lung tissue sections (Fig. 4). At week 9, the number and size of the lung masses increased in mice treated with the isotype control antibody and in those treated with α-mPD-1 in combination with GEM when compared with the number and size of lung masses observed in S2 mice at week 5 (Fig. 3).

As shown in Table 2, histopathological analysis with H&E-stained sections revealed the presence of adenomas in the lungs of all untreated mice (S2) at week 5, all mice treated with isotype control (G3) at week 9, and all mice treated with α-mPD-1 combined with GEM (G4) at week 9.

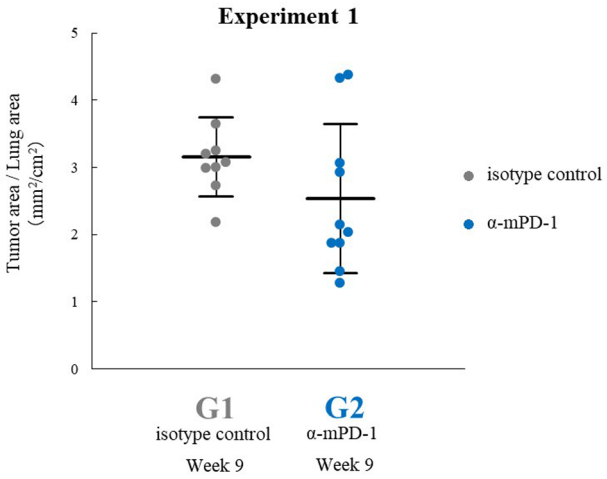

Fig. 2. Relative tumor areas in the lungs of the mice treated with the isotype control antibody (Group 1) and α-mPD-1 (Group 2). Data are expressed as the mean (bars) ± standard deviation (S.D.) (error bars) for each group. Dots represent individual animal values. The difference in tumor area between the two groups is not statistically significant. α-mPD-1, anti-mouse PD-1 antibody.

Table 3. Relative Lung Tumor Area Measured by Image Analysis in Experiments 1 and 2

Expt.	Group	Treatment	No. of mice	No. of lung section examined	Necropsy at week	Lung area (mm^2)	Tumor area (mm^2)	Tumor area/ Lung area (mm^2/cm^2)
1	S1	-	2	-[a]	5	-[a]	-[a]	-[a]
	G1	Isotype control	9	21.6 ± 0.7[b]	9	93.91 ± 6.29[b]	2.96 ± 0.58[b]	3.15 ± 0.59[b]
	G2	α-mPD-1	10	21.8 ± 0.4	9	99.91 ± 7.39	2.50 ± 1.04	2.54 ± 1.11
2	S2	-	12	22.0 ± 0.4	5	86.21 ± 8.97	0.78 ± 0.48	0.94 ± 0.68
	G3	Isotype control	8	21.6 ± 0.9	9	98.60 ± 7.34	6.22 ± 3.01	6.22 ± 2.64
	G4	α-mPD-1 + GEM	8	22.1 ± 0.4	9	103.98 ± 7.30	3.68 ± 1.52*	3.52 ± 1.35*

a: Only tumor expression was confirmed, b: Mean ± SD. *p<0.05 compared to Group 3 with Student's t-test.
All mice were administered ENU+BHT as initiation/promotion protocol.

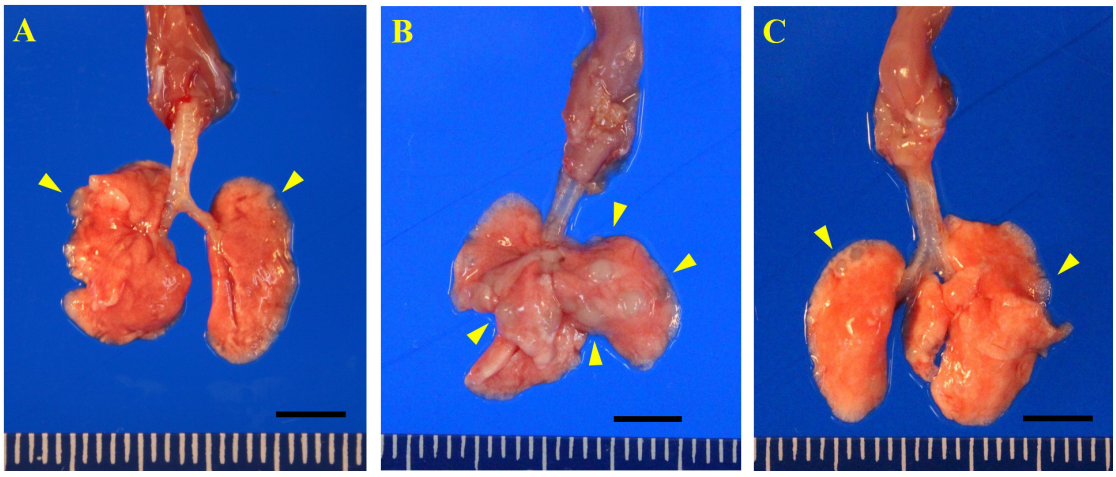

Fig. 3. Lung images from lung carcinogenesis model mice in Experiment 2. Gross pathology shows nodular masses in the lungs (arrowhead) of untreated mice at week 5 (Panel A), mice treated with isotype control at week 9 (Panel B), and those treated with α-mPD-1 in combination with GEM at week 9 (Panel C). Bar=5 mm. α-mPD-1, anti-mouse PD-1 antibody; GEM, gemcitabine.

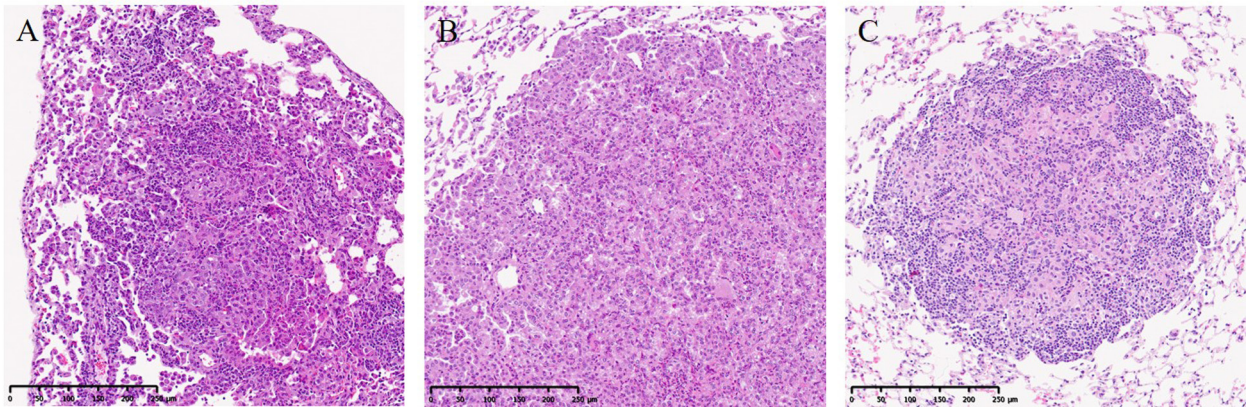

Fig. 4. Hematoxylin-eosin-stained lung tissue specimens of untreated mice at week 5 (Panel A), mice treated with isotype control antibodies at week 9 (Panel B), and mice treated with a combination of α-mPD-1 and GEM at week 9 (Panel C) showing that typical adenomas developed in the lungs of these animals. α-mPD-1, anti-mouse PD-1 antibody; GEM, gemcitabine.

The typical histopathology of adenomas in the lungs of each group is shown in Fig. 4. Immunostaining with anti-PD-L1 antibody (Fig. 5) indicated the presence of programmed death-ligand 1 (PD-L1; also known as CD274 and B7-H1) in adenomas and/or immune cells, suggesting that these adenomas are potentially responsive to α-mPD-1 treatment[25, 26]. Individual differences in tumor PD-L1 expression were noted, and even within the same individual animals that expressed PD-L1, differences in tumor expression could be observed.

At the end of week 9, the tumor area was significantly smaller in mice treated with the combination of α-mPD-1 and GEM than in isotype control mice ($p<0.05$; 6.22 and 3.52 mm^2/cm^2 in isotype control mice and mice treated with α-mPD-1 and GEM, respectively) (Fig. 6 and Table 3).

Discussion

It has been reported that lung adenomas can be detected at week 9 in the rasH2/BHT model used to detect genotoxic lung carcinogens, including ENU[13]. In the present study, bronchioloalveolar adenomas were identified at week 5 in all rasH2 mice treated with ENU and BHT. Following immunohistochemical analysis, we noted PD-L1 expression in adenomas or immune cells, indicating that these tumors are potentially responsive to α-mPD-1[25, 26]. However, treatment with α-mPD-1 for 4 weeks failed to demonstrate statistically significant antitumor efficacy in this model. Conversely, mice treated with a combination of α-mPD-1 and GEM exhibited a statistically significant antitumor effect. Importantly, all mice treated with combined α-mPD-1 and GEM presented smaller relative tumor areas than the mean values of the control group, supporting the hypothesis that combination therapy could inhibit tumor growth.

The NOAEL (no-observed-adverse-effect level) of therapeutic drugs used in the present study was 200 mg/kg/week for αPD-1 (5 times, i.v., cynomolgus monkeys)[27] and 40 mg/kg/week for GEM (3 months, i.p. B6C3F1 mouse)[28]. The doses employed in our model were approximately one-tenth (α-mPD-1) and one-quarter (GEM) of the NOAEL dose, with no documented signs of toxicity.

The absence or presence and degree of PD-L1 expression in tumors were heterogeneous, suggesting that the drug efficacy of α-mPD-1, a PD-L1 antagonist, did not significantly differ when administered as a single agent: it was likely more effective in tumors expressing higher levels of PD-L1 and less effective in tumors expressing lower levels of PD-L1. In combination therapy, low concentrations of GEM could decrease immunosuppressive cells, such as Treg cells (Tregs) and MDSCs in the tumor microenvironment[17, 29, 30], thereby increasing tumor immunogenicity[31]. Consequently, tumor-infiltrating lymphocytes (TILs) are elevated, and TIL-secreted cytokines, such as interferon (IFN)-γ, act on the tumor and enhance PD-L1 expression[32]. PD-1 activation is associated with exhaustion of cytotoxic T lymphocytes[33–35]. Anti-PD-1 antibodies act as follows: antibody blockade of the PD-L1-PD-1 pathway reverses cytotoxic T cell exhaustion, with combination therapy with GEM and α-PD-1 potentially inducing a synergistic effect.

As noted above, we used one-quarter of the NOAEL dose of GEM. However, the toxicity of GEM must be monitored. GEM-mediated toxicity includes leukopenia and suppression of weight gain[28]. Concomitant administration of 90 mg/kg GEM, which is close to the maximal tolerable dose[36], reduces cytotoxic T lymphocytes owing to its toxicity[31], abolishing the synergistic effect of combination treatment with GEM and anti-PD-1 antibody. However, with proper management, combination therapy with GEM and anti-PD-1 antibody can be effective. Herein, combination therapy with GEM significantly impacted anti-PD-1 antibody antitumor activity, such that an antitumor effect was detectable in most, or all, treated mice.

In a mesothelioma preclinical model using subcutaneous implantation of RN5 tumors in syngeneic mice, GEM plus anti-CTLA4 plus anti-PD1 outperformed GEM alone and anti-CTLA-4 plus anti-PD1 alone. Two patients who

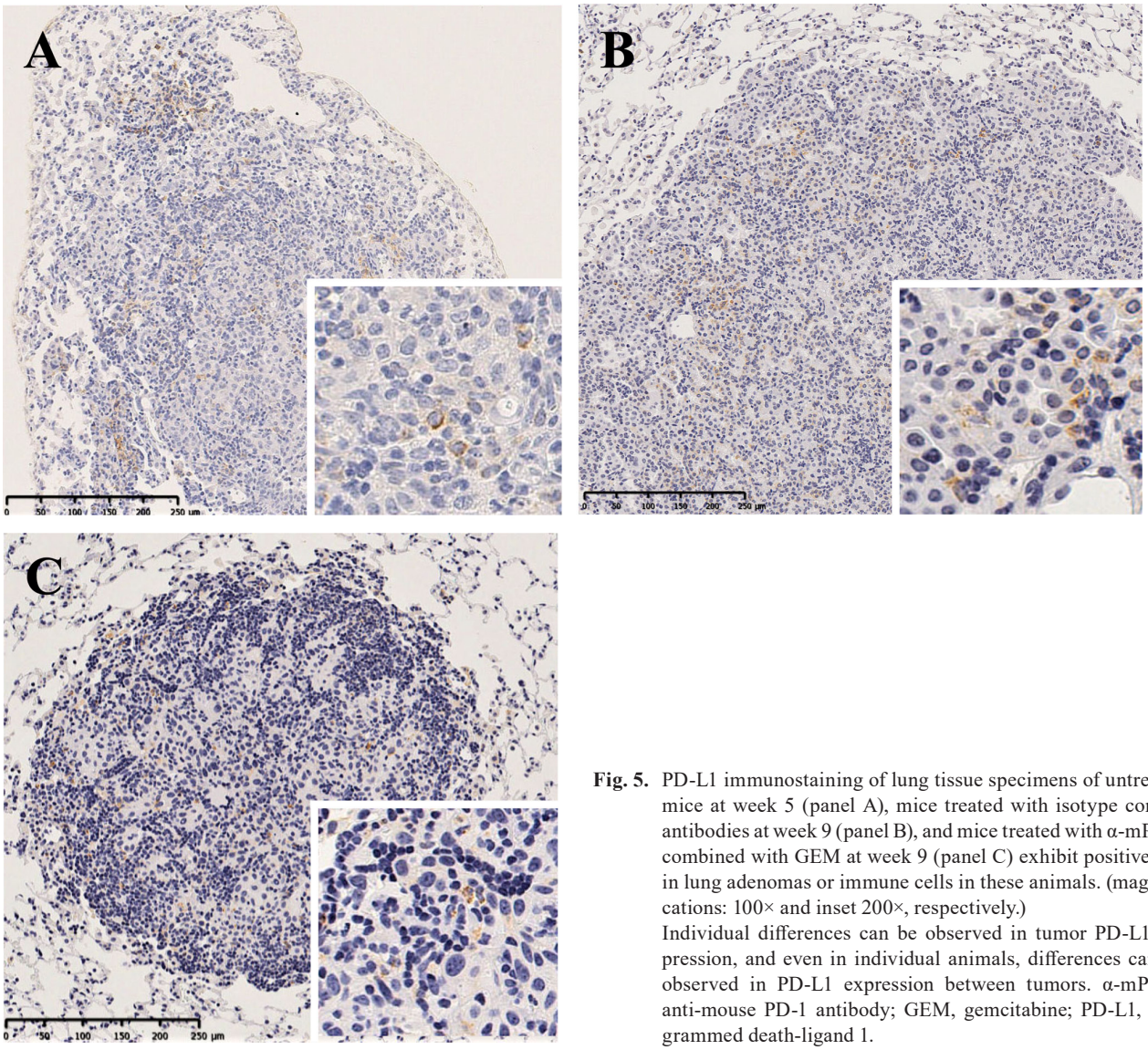

Fig. 5. PD-L1 immunostaining of lung tissue specimens of untreated mice at week 5 (panel A), mice treated with isotype control antibodies at week 9 (panel B), and mice treated with α-mPD-1 combined with GEM at week 9 (panel C) exhibit positive site in lung adenomas or immune cells in these animals. (magnifications: 100× and inset 200×, respectively.)
Individual differences can be observed in tumor PD-L1 expression, and even in individual animals, differences can be observed in PD-L1 expression between tumors. α-mPD-1, anti-mouse PD-1 antibody; GEM, gemcitabine; PD-L1, programmed death-ligand 1.

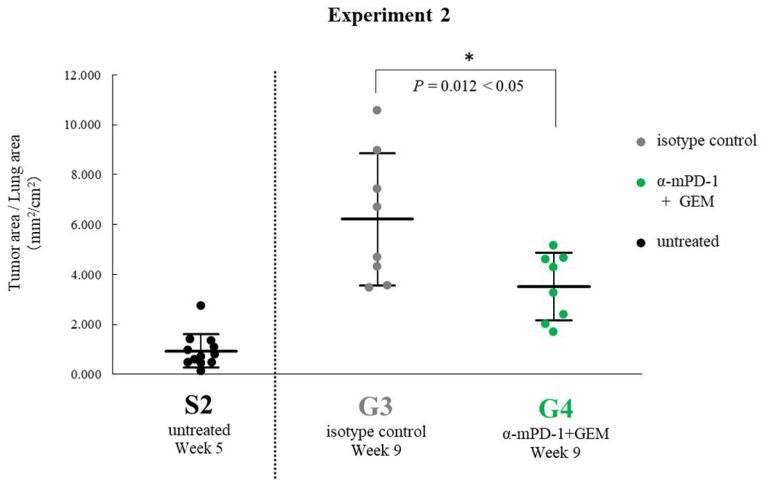

Fig. 6. Relative tumor area in lungs of mice treated with isotype control antibody (Group 3: G3) and a combination of α-mPD-1 with GEM (Group 4: G4) and untreated mice (Satellite group 2: S2). Data are expressed as the mean (bars) ± standard deviation (S.D.) (error bars) for each group. Dots represent individual animal values. *p<0.05, compared to Group 3 using Student's t-test. α-mPD-1, anti-mouse PD-1 antibody; GEM, gemcitabine.

failed to respond to pembrolizumab (anti-PD-1) or GEM monotherapy were treated with a combination of GEM and anti-PD-1, and both exhibited a positive clinical response to combination therapy. However, disease progression was detected in one patient and treatment was discontinued; the second patient continued therapy[18]. The ORIENT-12 phase III clinical trial also concluded that combining sintilimab (anti-PD-1) with GEM and a platinum-based chemotherapy drug as first-line treatment for locally advanced or metastatic squamous cell lung carcinoma is a feasible therapeutic option[37, 38]. The results of lung tumor treatment in our mouse model were analogous to those in human patients. In an orthotopic lung cancer model using the murine Lewis lung carcinoma cell line and C57BL/6 mice, a significant decrease in CD8 + and CD4 + T cells was noted as MDSCs increased along with lung tumor volume. Administration of GEM in this model suppressed the number of MDSCs and significantly prolonged survival[39]. Compared with healthy donors, a significantly increased frequency of circulating monocytic (M)-MDSCs was observed in patients with NSCLC. Furthermore, the frequency of M-MDSCs and polymorphonuclear (PMN)-MDSCs was higher in the tumor than in the peripheral blood of the same patients[40]. In a meta-analysis of studies assessing patients with various solid tumors (e.g., colon, liver, and stomach cancers), MDSCs were significantly associated with overall survival and progression-free survival (PFS). MDSCs appear to play an important role in tumor growth and contribute to limiting the efficacy of anticancer therapy[41]. Patients with oral squamous cell carcinoma exhibit significantly higher levels of PMN-MDSCs than healthy controls. In the co-culture assay, the addition of PMN-MDSCs inhibited T cell proliferation and IFN-γ production[42]. Circulating $S100A9^+$ MDSCs can predict shorter PFS in patients with epidermal growth factor receptor (EGFR)-mutated lung adenocarcinoma[43]. Positivity for PD-L1, the ligand for anti-PD-1 antibodies in patients with lung adenocarcinoma and lung squamous cell carcinoma, is reportedly higher in patients with lung adenocarcinoma[44]. Thus, regardless of the histopathologic morphology of NSCLC, squamous cell lung carcinoma, or lung adenocarcinoma, GEM reduces MDSCs that inhibit T cell function and may contribute to the synergistic effect of anticancer therapy when administered in combination with an anti-PD-1 antibody.

In patients treated with combined anti-PD-1 and GEM, the dose of GEM was higher (up to 27 mg/kg)[18, 37, 38, 45] than that used in the present study. The sensitivity of our mouse model to relatively low doses of GEM is consistent with the fact that this low GEM dose was sufficiently high to reduce immunosuppressive Tregs and MDSC tumor infiltration[17, 29]. Combining a GEM dose that can inhibit tumor infiltration and subsequent immunosuppression by Treg cells and MDSCs, which partly act via the PD-1 pathway, coupled with direct suppression by α-mPD-1 of PD-1, could afford an additive effect on the suppression of PD-1-mediated immune evasion mechanisms; this effect is further enhanced by reversal of cytotoxic T cell exhaustion. The results of the present study support the importance of combination therapies for treating patients with lung cancer using ICIs.

As noted above, adenoma development in this model varies and leads to individual variations in response to the tested therapies, which is the expected therapeutic outcome in humans. It is likely that treatment with α-mPD-1 exhibited an antitumor effect in some mice but not in others; this is also the human response to α-mPD-1 and other ICI therapies. The superior antitumor effect mediated by combination therapy over α-mPD-1 monotherapy, likely to occur in most patients, suggests that this model has the potential for preclinical testing of optimal doses and combinations of various anticancer agents.

Herein, we employed transgenic mice carrying the c-Ha-ras gene, a human proto-oncogene; therefore, it is expected that the lung tumors in our model will carry human H-ras mutations. However, the incidence of K-ras mutations in human lung adenocarcinomas is reportedly 25%[46], suggesting that adenomas developed in the present study may not precisely mimic those in humans. Nevertheless, in the often-used xenograft model, the drug efficacy of PD-1 monotherapy remains inconsistent[19–23, 26, 47, 48] owing to differences in PD-L1 expression of transplanted tumor cell lines[49–51] and the tumor microenvironment of the transplantation site[4, 52–54]. Compared with the results of the xenograft model, the rasH2/ENU/BHT model could potentially predict clinical outcomes with much greater confidence, given that the lung tumor microenvironment is autologous and spontaneous in origin, the host has an intact immune system response maintained by organ-specific tumorigenesis, and PD-L1 expression in lung tumors varies between individuals and even within the same individual, with differences in expression distribution resembling that reported in clinical practice[44, 55–58].

In conclusion, we showed that the response of a newly constructed chemical carcinogenesis model in transgenic mice to α-mPD-1 monotherapy and α-mPD-1 with GEM combination therapy strongly resembles results documented in human subjects. This model has the potential for preclinical testing of optimal doses and combinations of various anticancer agents.

Dislosure of Potential Conflicts of Interest: The authors declare no conflicts of interest associated with this manuscript.

Acknowledgment: The authors thank Dr. David B. Alexander from Nagoya City University for reviewing our manuscript.

References

1. Fitzmaurice C, Dicker D, Pain A, Hamavid H, Moradi-Lakeh M, MacIntyre MF, Allen C, Hansen G, Woodbrook R, Wolfe C, Hamadeh RR, Moore A, Werdecker A, Gessner BD, Te Ao B, McMahon B, Karimkhani C, Yu C, Cooke GS, Schwebel DC, Carpenter DO, Pereira DM, Nash D, Kazi

DS, De Leo D, Plass D, Ukwaja KN, Thurston GD, Yun Jin K, Simard EP, Mills E, Park EK, Catalá-López F, deVeber G, Gotay C, Khan G, Hosgood HD 3rd, Santos IS, Leasher JL, Singh J, Leigh J, Jonas JB, Sanabria J, Beardsley J, Jacobsen KH, Takahashi K, Franklin RC, Ronfani L, Montico M, Naldi L, Tonelli M, Geleijnse J, Petzold M, Shrime MG, Younis M, Yonemoto N, Breitborde N, Yip P, Pourmalek F, Lotufo PA, Esteghamati A, Hankey GJ, Ali R, Lunevicius R, Malekzadeh R, Dellavalle R, Weintraub R, Lucas R, Hay R, Rojas-Rueda D, Westerman R, Sepanlou SG, Nolte S, Patten S, Weichenthal S, Abera SF, Fereshtehnejad SM, Shiue I, Driscoll T, Vasankari T, Alsharif U, Rahimi-Movaghar V, Vlassov VV, Marcenes WS, Mekonnen W, Melaku YA, Yano Y, Artaman A, Campos I, MacLachlan J, Mueller U, Kim D, Trillini M, Eshrati B, Williams HC, Shibuya K, Dandona R, Murthy K, Cowie B, Amare AT, Antonio CA, Castañeda-Orjuela C, van Gool CH, Violante F, Oh IH, Deribe K, Soreide K, Knibbs L, Kereselidze M, Green M, Cardenas R, Roy N, Tillmann T, Li Y, Krueger H, Monasta L, Dey S, Sheikhbahaei S, Hafezi-Nejad N, Kumar GA, Sreeramareddy CT, Dandona L, Wang H, Vollset SE, Mokdad A, Salomon JA, Lozano R, Vos T, Forouzanfar M, Lopez A, Murray C, Naghavi M. Global Burden of Disease Cancer Collaboration The global burden of cancer 2013. JAMA Oncol. **1**: 505–527. 2015. [Medline] [CrossRef]

2. Hirsch FR, Scagliotti GV, Mulshine JL, Kwon R, Curran WJ Jr, Wu YL, and Paz-Ares L. Lung cancer: current therapies and new targeted treatments. Lancet. **389**: 299–311. 2017. [Medline] [CrossRef]
3. Steven A, Fisher SA, and Robinson BW. Immunotherapy for lung cancer. Respirology. **21**: 821–833. 2016. [Medline] [CrossRef]
4. Devaud C, Westwood JA, John LB, Flynn JK, Paquet-Fifield S, Duong CP, Yong CS, Pegram HJ, Stacker SA, Achen MG, Stewart TJ, Snyder LA, Teng MW, Smyth MJ, Darcy PK, and Kershaw MH. Tissues in different anatomical sites can sculpt and vary the tumor microenvironment to affect responses to therapy. Mol Ther. **22**: 18–27. 2014. [Medline] [CrossRef]
5. Daniel VC, Marchionni L, Hierman JS, Rhodes JT, Devereux WL, Rudin CM, Yung R, Parmigiani G, Dorsch M, Peacock CD, and Watkins DN. A primary xenograft model of small-cell lung cancer reveals irreversible changes in gene expression imposed by culture in vitro. Cancer Res. **69**: 3364–3373. 2009. [Medline] [CrossRef]
6. Yu JW, Bhattacharya S, Yanamandra N, Kilian D, Shi H, Yadavilli S, Katlinskaya Y, Kaczynski H, Conner M, Benson W, Hahn A, Seestaller-Wehr L, Bi M, Vitali NJ, Tsvetkov L, Halsey W, Hughes A, Traini C, Zhou H, Jing J, Lee T, Figueroa DJ, Brett S, Hopson CB, Smothers JF, Hoos A, and Srinivasan R. Tumor-immune profiling of murine syngeneic tumor models as a framework to guide mechanistic studies and predict therapy response in distinct tumor microenvironments. PLoS One. **13**: e0206223. 2018. [Medline] [CrossRef]
7. Scarlett C, Weidenhofer J, Colvin E, and Bond D. Animal models of pancreatic cancer and their application in clinical research. Gastrointest Cancer. **6**: 31–39. 2016.
8. Mak IW, Evaniew N, and Ghert M. Lost in translation: animal models and clinical trials in cancer treatment. Am J Transl Res. **6**: 114–118. 2014. [Medline]
9. Jacobs AC, and Brown PC. Regulatory forum opinion piece*: transgenic/alternative carcinogenicity assays: a retrospective review of studies submitted to CDER/FDA 1997–2014. Toxicol Pathol. **43**: 605–610. 2015. [Medline] [CrossRef]
10. Shibuya T, and Morimoto K. A review of the genotoxicity of 1-ethyl-1-nitrosourea. Mutat Res. **297**: 3–38. 1993. [Medline] [CrossRef]
11. The 15th Report on Carcinogens; N-Nitrosamines: 15 Listings. 2021, from National Toxicology Program (NTP) website: https://ntp.niehs.nih.gov/ntp/roc/content/profiles/nitrosamines.pdf.
12. Umemura T, Kodama Y, Hioki K, Nomura T, Nishikawa A, Hirose M, and Kurokawa Y. The mouse rasH2/BHT model as an in vivo rapid assay for lung carcinogens. Jpn J Cancer Res. **93**: 861–866. 2002. [Medline] [CrossRef]
13. Umemura T, Kodama Y, Nishikawa A, Hioki K, Nomura T, Kanki K, Kuroiwa Y, Ishii Y, Kurokawa Y, and Hirose M. Nine-week detection of six genotoxic lung carcinogens using the rasH2/BHT mouse model. Cancer Lett. **231**: 314–318. 2006. [Medline] [CrossRef]
14. NTP Bioassay of Butylated Hydroxytoluene (BHT) for Possible Carcinogenicity (CASRN 128-37-0), National Toxicology Program, Public Health Service, U.S. Department of Health and Human Services; NTP TR-150. 1979, from National Toxicology Program (NTP) website: https://ntp.niehs.nih.gov/publications/reports/tr/100s/tr150/index.html.
15. Toschi L, and Cappuzzo F. Gemcitabine for the treatment of advanced nonsmall cell lung cancer. OncoTargets Ther. **2**: 209–217. 2009. [Medline]
16. Yang Z, Guo J, Weng L, Tang W, Jin S, and Ma W. Myeloid-derived suppressor cells-new and exciting players in lung cancer. J Hematol Oncol. **13**: 10. 2020. [Medline] [CrossRef]
17. Vincent J, Mignot G, Chalmin F, Ladoire S, Bruchard M, Chevriaux A, Martin F, Apetoh L, Rébé C, and Ghiringhelli F. 5-Fluorouracil selectively kills tumor-associated myeloid-derived suppressor cells resulting in enhanced T cell-dependent antitumor immunity. Cancer Res. **70**: 3052–3061. 2010. [Medline] [CrossRef]
18. Tallón de Lara P, Cecconi V, Hiltbrunner S, Yagita H, Friess M, Bode B, Opitz I, Vrugt B, Weder W, Stolzmann P, Felley-Bosco E, Stahel RA, Tischler V, Britschgi C, Soldini D, van den Broek M, and Curioni-Fontecedro A. Gemcitabine synergizes with immune checkpoint inhibitors and overcomes resistance in a preclinical model and mesothelioma patients. Clin Cancer Res. **24**: 6345–6354. 2018. [Medline] [CrossRef]
19. Juneja VR, McGuire KA, Manguso RT, LaFleur MW, Collins N, Haining WN, Freeman GJ, and Sharpe AH. PD-L1 on tumor cells is sufficient for immune evasion in immunogenic tumors and inhibits CD8 T cell cytotoxicity. J Exp Med. **214**: 895–904. 2017. [Medline] [CrossRef]
20. Grasselly C, Denis M, Bourguignon A, Talhi N, Mathe D, Tourette A, Serre L, Jordheim LP, Matera EL, and Dumontet C. The antitumor activity of combinations of cytotoxic chemotherapy and immune checkpoint inhibitors is model-dependent. Front Immunol. **9**: 2100. 2018. [Medline] [CrossRef]
21. Chen S, Lee LF, Fisher TS, Jessen B, Elliott M, Evering W, Logronio K, Tu GH, Tsaparikos K, Li X, Wang H, Ying C, Xiong M, VanArsdale T, and Lin JC. Combination of

4-1BB agonist and PD-1 antagonist promotes antitumor effector/memory CD8 T cells in a poorly immunogenic tumor model. Cancer Immunol Res. **3**: 149–160. 2015. [Medline] [CrossRef]
22. Arlauckas SP, Garris CS, Kohler RH, Kitaoka M, Cuccarese MF, Yang KS, Miller MA, Carlson JC, Freeman GJ, Anthony RM, Weissleder R, and Pittet MJ. In vivo imaging reveals a tumor-associated macrophage-mediated resistance pathway in anti-PD-1 therapy. Sci Transl Med. **9**: 9. 2017. [Medline] [CrossRef]
23. Cooper ZA, Juneja VR, Sage PT, Frederick DT, Piris A, Mitra D, Lo JA, Hodi FS, Freeman GJ, Bosenberg MW, McMahon M, Flaherty KT, Fisher DE, Sharpe AH, and Wargo JA. Response to BRAF inhibition in melanoma is enhanced when combined with immune checkpoint blockade. Cancer Immunol Res. **2**: 643–654. 2014. [Medline] [CrossRef]
24. Efficacy of J43 and gemcitabine in combination in MC38 allogeneic tumor models: Merck & Co., KEYTRUDA® Injection, Common Technical Document. 2016, from the Pharmaceuticals and Medical Devices Agency (PMDA), Japan website: https://www.pmda.go.jp/drugs/2016/P20161025002/170050000_22800AMX00696000_H100_1.pdf.
25. Teixidó C, Vilariño N, Reyes R, and Reguart N. PD-L1 expression testing in non-small cell lung cancer. Ther Adv Med Oncol. **10**: 1758835918763493. 2018. [Medline] [CrossRef]
26. Lau J, Cheung J, Navarro A, Lianoglou S, Haley B, Totpal K, Sanders L, Koeppen H, Caplazi P, McBride J, Chiu H, Hong R, Grogan J, Javinal V, Yauch R, Irving B, Belvin M, Mellman I, Kim JM, and Schmidt M. Tumour and host cell PD-L1 is required to mediate suppression of anti-tumour immunity in mice. Nat Commun. **8**: 14572. 2017. [Medline] [CrossRef]
27. One-month intravenous toxicity study in cynomolgus monkey, MK-3475, Merck & Co. Pembrolizumab Common Technical Document. 2016, website: https://www.pmda.go.jp/drugs/2016/P20161025002/170050000_22800AMX00696000_J100_1.pdf.
28. Items related to non-clinical studies, repeated dose toxicity studies, pharmaceutical interview form (IF), Gemzar® Injection, Eli Lilly Japan K.K. 2019, website: https://www.info.pmda.go.jp/go/interview/1/530471_4224403D1030_1_2F.pdf.
29. Shevchenko I, Karakhanova S, Soltek S, Link J, Bayry J, Werner J, Umansky V, and Bazhin AV. Low-dose gemcitabine depletes regulatory T cells and improves survival in the orthotopic Panc02 model of pancreatic cancer. Int J Cancer. **133**: 98–107. 2013. [Medline] [CrossRef]
30. Suzuki E, Kapoor V, Jassar AS, Kaiser LR, and Albelda SM. Gemcitabine selectively eliminates splenic Gr-1+/CD11b+ myeloid suppressor cells in tumor-bearing animals and enhances antitumor immune activity. Clin Cancer Res. **11**: 6713–6721. 2005. [Medline] [CrossRef]
31. Zhang X, Wang D, Li Z, Jiao D, Jin L, Cong J, Zheng X, and Xu L. Low-dose gemcitabine treatment enhances immunogenicity and natural killer cell-driven tumor immunity in lung cancer. Front Immunol. **11**: 331. 2020. [Medline] [CrossRef]
32. Abiko K, Matsumura N, Hamanishi J, Horikawa N, Murakami R, Yamaguchi K, Yoshioka Y, Baba T, Konishi I, and Mandai M. IFN-γ from lymphocytes induces PD-L1 expression and promotes progression of ovarian cancer. Br J Cancer. **112**: 1501–1509. 2015. [Medline] [CrossRef]
33. Woroniecka K, Chongsathidkiet P, Rhodin K, Kemeny H, Dechant C, Farber SH, Elsamadicy AA, Cui X, Koyama S, Jackson C, Hansen LJ, Johanns TM, Sanchez-Perez L, Chandramohan V, Yu YA, Bigner DD, Giles A, Healy P, Dranoff G, Weinhold KJ, Dunn GP, and Fecci PE. T-cell exhaustion signatures vary with tumor type and are severe in glioblastoma. Clin Cancer Res. **24**: 4175–4186. 2018. [Medline] [CrossRef]
34. Wherry EJ. T cell exhaustion. Nat Immunol. **12**: 492–499. 2011. [Medline] [CrossRef]
35. Ando M, Ito M, Srirat T, Kondo T, and Yoshimura A. Memory T cell, exhaustion, and tumor immunity. Immunol Med. **43**: 1–9. 2020. [Medline] [CrossRef]
36. van Moorsel CJ, Pinedo HM, Veerman G, Vermorken JB, Postmus PE, and Peters GJ. Scheduling of gemcitabine and cisplatin in Lewis lung tumour bearing mice. Eur J Cancer. **35**: 808–814. 1999. [Medline] [CrossRef]
37. Zhou C, Wu L, Fan Y, Wang Z, Liu L, Chen G, Zhang L, Huang D, Cang S, Yang Z, Zhou J, Zhou C, Li B, Li J, Fan M, Cui J, Li Y, Zhao H, Fang J, Xue J, Hu C, Sun P, Du Y, Zhou H, Wang S, and Zhang W. Sintilimab plus platinum and gemcitabine as first-line treatment for advanced or metastatic squamous NSCLC: results from a randomized, double-blind, phase 3 trial (ORIENT-12). J Thorac Oncol. **16**: 1501–1511. 2021. [Medline] [CrossRef]
38. Zhou CWL, Fan Y, Wang Z, Liu L, Chen G, Zhang L, Huang D, Cang S, Yang Z, Zhou J, Zhou C, Li B, Li J, Fan M, Zhang W, Yang W, Wang S, and Zhou H. LBA56 ORIENT-12: Sintilimab plus gemcitabine and platinum (GP) as first-line (1L) treatment for locally advanced or metastatic squamous non-small-cell lung cancer (sqNSCLC). Ann Oncol. **31**: S1186. 2020.
39. Sawant A, Schafer CC, Jin TH, Zmijewski J, Tse HM, Roth J, Sun Z, Siegal GP, Thannickal VJ, Grant SC, Ponnazhagan S, and Deshane JS. Enhancement of antitumor immunity in lung cancer by targeting myeloid-derived suppressor cell pathways. Cancer Res. **73**: 6609–6620. 2013. [Medline] [CrossRef]
40. Yamauchi Y, Safi S, Blattner C, Rathinasamy A, Umansky L, Juenger S, Warth A, Eichhorn M, Muley T, Herth FJF, Dienemann H, Platten M, Beckhove P, Utikal J, Hoffmann H, and Umansky V. Circulating and tumor myeloid-derived suppressor cells in resectable non-small cell lung cancer. Am J Respir Crit Care Med. **198**: 777–787. 2018. [Medline] [CrossRef]
41. Zhang S, Ma X, Zhu C, Liu L, Wang G, and Yuan X. The role of myeloid-derived suppressor cells in patients with solid tumors: a meta-analysis. PLoS One. **11**: e0164514. 2016. [Medline] [CrossRef]
42. Zhong LM, Liu ZG, Zhou X, Song SH, Weng GY, Wen Y, Liu FB, Cao DL, and Liu YF. Expansion of PMN-myeloid derived suppressor cells and their clinical relevance in patients with oral squamous cell carcinoma. Oral Oncol. **95**: 157–163. 2019. [Medline] [CrossRef]
43. Feng P-H, Yu C-T, Chen K-Y, Luo C-S, Wu SM, Liu C-Y, Kuo LW, Chan Y-F, Chen T-T, Chang C-C, Lee C-N, Chuang H-C, Lin C-F, Han C-L, Lee W-H, and Lee K-Y. S100A9^{+} MDSC and TAM-mediated EGFR-TKI resistance in lung adenocarcinoma: the role of *RELB*. Oncotarget. **9**: 7631–7643. 2018. [Medline] [CrossRef]
44. D'Incecco A, Andreozzi M, Ludovini V, Rossi E, Capo-

danno A, Landi L, Tibaldi C, Minuti G, Salvini J, Coppi E, Chella A, Fontanini G, Filice ME, Tornillo L, Incensati RM, Sani S, Crinò L, Terracciano L, and Cappuzzo F. PD-1 and PD-L1 expression in molecularly selected non-small-cell lung cancer patients. Br J Cancer. **112**: 95–102. 2015. [Medline] [CrossRef]

45. Estimating the Maximum Safe Starting Dose in Initial Clinical Trials for Therapeutics in Adult Healthy Volunteers 2005. From website: https://www.fda.gov/media/72309/download.
46. Hirsch FR, Suda K, Wiens J, and Bunn PA Jr. New and emerging targeted treatments in advanced non-small-cell lung cancer. Lancet. **388**: 1012–1024. 2016. [Medline] [CrossRef]
47. Wei H, Zhao L, Li W, Fan K, Qian W, Hou S, Wang H, Dai M, Hellstrom I, Hellstrom KE, and Guo Y. Combinatorial PD-1 blockade and CD137 activation has therapeutic efficacy in murine cancer models and synergizes with cisplatin. PLoS One. **8**: e84927. 2013. [Medline] [CrossRef]
48. Dai M, Yip YY, Hellstrom I, and Hellstrom KE. Curing mice with large tumors by locally delivering combinations of immunomodulatory antibodies. Clin Cancer Res. **21**: 1127–1138. 2015. [Medline] [CrossRef]
49. Analysis of PD-L1 expression in various mouse tumors by quantitative IHC, avelumab (genetical recombination): Merck Serono Co., Ltd, Common Technical Document. 2017, from the Pharmaceuticals and Medical Devices Agency (PMDA), Japan website: https://www.pmda.go.jp/drugs/2017/P20171024003/380079000_22900AMX00990000_H100_1.pdf.
50. Grenga I, Donahue RN, Lepone L, Bame J, Schlom J, and Farsaci B. PD-L1 and MHC-I expression in 19 human tumor cell lines and modulation by interferon-gamma treatment. J Immunother Cancer. **2**: 102. 2014. [CrossRef]
51. CD274 molecule, Cancer Cell Line Encyclopedia (CCLE) dataset, The DepMap project at the Broad Institute. website: https://depmap.org/portal/gene/CD274?tab=dependency&dependency=Chronos_Combined.
52. Li HY, McSharry M, Bullock B, Nguyen TT, Kwak J, Poczobutt JM, Sippel TR, Heasley LE, Weiser-Evans MC, Clambey ET, and Nemenoff RA. The tumor microenvironment regulates sensitivity of murine lung tumors to PD-1/PD-L1 antibody blockade. Cancer Immunol Res. **5**: 767–777. 2017. [Medline] [CrossRef]
53. Zhan B, Wen S, Lu J, Shen G, Lin X, Feng J, and Huang H. Identification and causes of metabonomic difference between orthotopic and subcutaneous xenograft of pancreatic cancer. Oncotarget. **8**: 61264–61281. 2017. [Medline] [CrossRef]
54. Oliver AJ, Lau PKH, Unsworth AS, Loi S, Darcy PK, Kershaw MH, and Slaney CY. Tissue-dependent tumor microenvironments and their impact on immunotherapy responses. Front Immunol. **9**: 70. 2018. [Medline] [CrossRef]
55. McLaughlin J, Han G, Schalper KA, Carvajal-Hausdorf D, Pelekanou V, Rehman J, Velcheti V, Herbst R, LoRusso P, and Rimm DL. Quantitative assessment of the heterogeneity of PD-L1 expression in non-small-cell lung cancer. JAMA Oncol. **2**: 46–54. 2016. [Medline] [CrossRef]
56. Pan Y, Zheng D, Li Y, Cai X, Zheng Z, Jin Y, Hu H, Cheng C, Shen L, Wang J, Ji H, Sun Y, Zhou X, and Chen H. Unique distribution of programmed death ligand 1 (PD-L1) expression in East Asian non-small cell lung cancer. J Thorac Dis. **9**: 2579–2586. 2017. [Medline] [CrossRef]
57. Chen Q, Fu YY, Yue QN, Wu Q, Tang Y, Wang WY, Wang YS, and Jiang LL. Distribution of PD-L1 expression and its relationship with clinicopathological variables: an audit from 1071 cases of surgically resected non-small cell lung cancer. Int J Clin Exp Pathol. **12**: 774–786. 2019. [Medline]
58. CD274 LUNG CANCER–Protein expression, from the Human Protein Atlas (HPA) website: https://www.proteinatlas.org/ENSG00000120217-CD274/pathology/lung+cancer#imid_20974402.